applied sciences

MDPI

Article

A Novel Adaptive Model Predictive Control Based Three-Phase Inverter Current Control Method

Mingyu Lei [1,2], Ying Zhang [1,2], Lexuan Meng [3], Yibo Wang [1,2,*], Zilong Yang [1,2] and Dufeng Cao [1,2]

1 Solar Thermal Technology and Photovoltaic System Laboratory, China Academy of Sciences, Beijing 100190, China; leimingyu@mail.iee.ac.cn (M.L.); zhangying2011@mail.iee.ac.cn (Y.Z.); yangzl@mail.iee.ac.cn (Z.Y.); caodufeng888@126.com (D.C.)
2 Institute of Electrical Engineering, Chinese Academy of Sciences, Beijing 100190, China
3 Independent Researcher, 72482 Västerås, Sweden; lexuan.meng@gmail.com
* Correspondence: wyb@mail.iee.ac.cn; Tel.: +86-136-7135-5662

Received: 17 September 2019; Accepted: 6 November 2019; Published: 11 December 2019



Abstract: This paper proposes a novel current control method based on Model Predictive Control (MPC) for three-phase inverters. The proposed method is based on an Adaptive MPC (A-MPC) with a PWM modulation. An innovative model parameter estimation and modification method is also proposed, leading to enhanced control accuracy. Comparing with traditional current control methods, such as PI and PR control, the proposed method has better dynamic performance. The transient dynamics, i.e., recovery time and overshoot, have been considerably improved. Simulation and experimental results are presented to validate the effectiveness of the proposal.

Keywords: Inverters; model predictive control; current control; dynamic performance

1. Introduction

Model Predictive Control (MPC) is recently regarded as one of the most promising control methods in controlling power converters, due to its predictive effect and robustness [1]. The fundamental idea of MPC is to predict the optimal controls of next step(s) to minimize the cost function based on the model of the object under control as well as a set of constraints. During normal operation, the accuracy of predicted model parameters can be improved online, resulting in enhanced control accuracy and better adaptability [2]. This feature is highly attractive when the operating conditions varies frequently.

In recent years, MPC has been successfully used in grid-tie converters for renewable energy systems, where it delivers improved dynamic performances, robustness and system stability [3–8]. In most of existing applications of MPC for power converters, the control command of next period is directly selected from a finite set of switching states according to the cost function, namely finite-control-set MPC (FCS-MPC) [9–12]. While in some other approaches, the output variables, such as the current or voltage references, are continuous values, and these methods are known as continuous control set MPC (CCS-MPC) [13,14].

Applications of FCS-MPC have attracted much attention because of several advantages, such as fast transient response, simple implementation, and so on. Up to now, most MPC based control methods for power converters are of this type. In [15], a FCS-MPC on three-phase voltage source inverter is proposed to select an optimal switching state for next step to minimize the error and guarantee control accuracy. Experimental results show that the proposed method controls the load currents effectively with a better dynamic response comparing to conventional linear control methods. In addition, this method is simple and easy for DSP implementation. Paper [16] proposes a FCS-MPC on controlling the flying capacitor voltage and the grid current of the Packed-U-Cells inverter. The eight available switching states are evaluated every

period and the optimal one is selected according to a cost function. Experimental results validate the good dynamic performance in controlling the grid-connected system. Paper [17] proposes a FCS-MPC based control method for four-leg indirect matrix converters to minimize the instantaneous reactive input power. A significant advantage of this method is the reduction of control strategy complexity.

However, FCS-MPC is not suitable in the cases when the optimal switching state cannot be directly selected or there are considerably number of switching states. The three major drawbacks of FCS-MPC are: (i) High computational burden due to evaluation of all the switching states; (ii) low control accuracy due to limited switching states; (iii) model dependency [13].

Paper [13] has validated that CCS-MPC based methods have better performance and reduced computational burden in power electronic system applications. In this paper, a CCS-MPC based control method for grid-connected photovoltaic (PV) systems. The proposed method is applied to control the power exchange between PV and grid, while achieving the unit power factor. It is verified to have good dynamic performance. In [18], a CCS-MPC method is applied in controlling of permanent magnet synchronous machines. Experimental results prove the effectiveness of the proposed method in such applications.

However, for above mentioned approaches, the performance of the control largely depends on the accuracy of the model parameters. An inherent steady-state error cannot be eliminated during the control process since there is no adaptation on the parameters. Paper [19] analyzes the influence of model error on the accuracy of MPC for current control in a three-phase inverter. It has been confirmed that the mismatch of prediction inductance can cause steady-state error in inverter current. Limited research works have been conducted in improving the model accuracy. In [20], an MPC based current control of a switched reluctance motor is proposed, in which an adaptive controller is used to dynamically estimate and modify the motor inductance based on Kalman Filter theory. Paper [21] proposes a FCS-MPC based control method for voltage source inverter. This method is able to correct the correct parameters based on ADALINE estimator. However, the adaptive methods proposed in [20,21] require additional algorithm installation and processing in controller, which inevitably increases the computational burden.

In this paper, an Adaptive Model Predictive Control (A-MPC) based three-phase inverter current control method is proposed. The most important contribution of this method is the novel parameter estimation and adapting algorithm, which is simple and efficient. The parameter estimation and modification method is decoupled with the current control loop. No extra control algorithm is used in this estimation method. The parameter estimation can improve the control accuracy. The optimal switching state components in two-phase rotating coordinate system is generated and used as the input for parameter estimation and modulation. Since the variables (e.g., voltages, currents, switching states and their references) are all DC components, the optimal switching state can be calculated directly, avoiding the evaluation of all the available switching states. Therefore, the computational burden is effectively reduced. Simulations and experiments validate the effectiveness of the proposed method and the enhancement in system performance.

2. Model of an Inverter

The main circuit of a full bridge AC/DC inverter studied in this work is shown in Figure 1. In this system, it is assumed that the system is balanced, and the DC voltage of the inverter is stable. The general mathematical model of this inverter can be obtained as [22]

$$\begin{cases} L\frac{di_a}{dt} + Ri_a + e_a = U_{DC}(S_a - \frac{S_a+S_b+S_c}{3}) \\ L\frac{di_b}{dt} + Ri_b + e_b = U_{DC}(S_b - \frac{S_a+S_b+S_c}{3}) \\ L\frac{di_c}{dt} + Ri_c + e_c = U_{DC}(S_c - \frac{S_a+S_b+S_c}{3}) \end{cases} \quad (1)$$

where L and R are the filter inductance and resistance respectively. The S_a, S_b and S_c are the switching state variables of the switching devices. The e_a, e_b, e_c are the phase voltages of the grid. This three-phase model can be also presented in a two-phase stationary coordinate system ($\alpha\beta$coordinate system). The transformation expression of the variables between these two coordinate systems is shown as following:

$$\begin{bmatrix} \alpha \\ \beta \end{bmatrix} = \frac{2}{3}\begin{bmatrix} 1 & -0.5 & -0.5 \\ 0 & \frac{\sqrt{3}}{2} & -\frac{\sqrt{3}}{2} \end{bmatrix}\begin{bmatrix} a \\ b \\ c \end{bmatrix} \tag{2}$$

By transforming all the variables to the two-phase stationary coordinate system, the mathematical model can be expressed as

$$\begin{cases} L\frac{di_\alpha}{dt} + Ri_\alpha + e_\alpha = \frac{2}{3}U_{DC}S_\alpha \\ L\frac{di_\beta}{dt} + Ri_\beta + e_\beta = \frac{2}{3}U_{DC}S_\beta \end{cases} \tag{3}$$

where S_α and S_β are the switching functions in two-phase stationary coordinate. In this modeling expression, the switching variables, current and voltage are still of AC system. The model can be transformed to the two-phase rotating coordinate system. The transformation expression between these two systems is defined as

$$\begin{bmatrix} d \\ q \end{bmatrix} = \begin{bmatrix} \cos\theta & \sin\theta \\ -\sin\theta & \cos\theta \end{bmatrix}\begin{bmatrix} \alpha \\ \beta \end{bmatrix} \tag{4}$$

By taking (4) into (3), the mathematical model of this inverter in two-phase rotating coordinate system is shown as followings:

$$\begin{cases} L\frac{di_d}{dt} + Ri_d = \omega Li_q - e_d + \frac{2}{3}U_{DC}S_d \\ L\frac{di_q}{dt} + Ri_q = -\omega Li_d - e_q + \frac{2}{3}U_{DC}S_q \end{cases} \tag{5}$$

where S_d and S_q are the switching functions in two-phase stationary coordinate. In this expression, all of the variables (e.g., current, voltage and switching states) are of DC system. The orientation of these systems are shown in Figure 2.

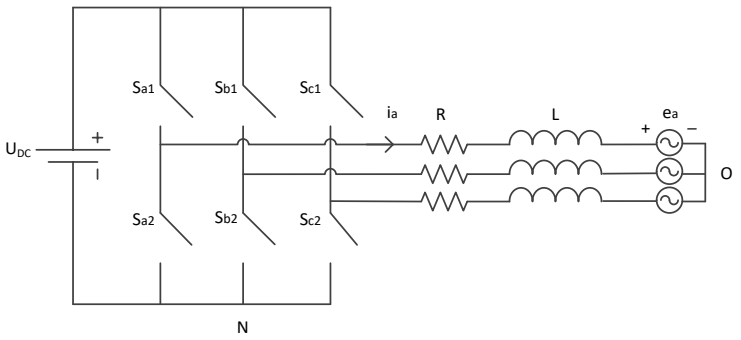


Figure 1. Structure of a three-phase inverter.

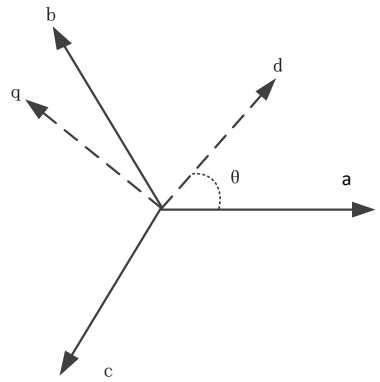


Figure 2. The orientation of *abc* and *dq* coordinate systems.

3. Adaptive Model Predictive Current Control for Inverters

The main idea of MPC is to predict the future states of the system under control and select the control variables minimizing the given cost function according to the predicted mathematical model. In this proposed A-MPC method, the model parameters can be updated online according to the error between the predicted and the actual output value. The main process of this control method is given in Figure 3.

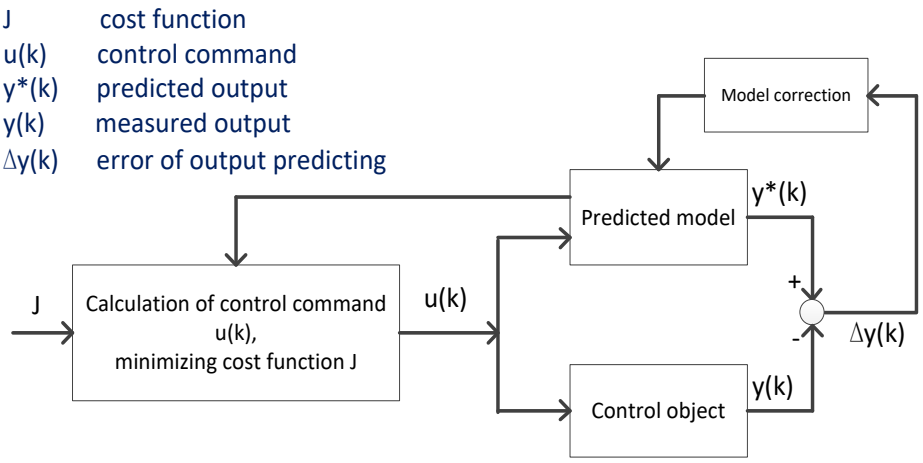


Figure 3. Main process of A-MPC current control method.

3.1. Selection of Switching States

The overall control scheme proposed in this paper can be divided into three steps: (i) Select the optimal switching state, (ii) apply the modulation, and (iii) adaptively modify the parameters. In this method, the mathematical model expression in *dq* coordinate system is employed. In order to calculate the optimal switching state, the cost function of MPC is given as

$$J = \left|i_{dref} - i_d(k+1)\right| + \left|i_{qref} - i_q(k+1)\right| \tag{6}$$

where i_{dref} and i_{qref} are the references of inverter output currents in two-phase rotating coordinate system. The output variables (y_1 and y_2) and control variables (u_1 and u_2) are defined as follows:

$$y = \begin{bmatrix} i_d \\ i_q \end{bmatrix} \quad , \quad u = \begin{bmatrix} S_d \\ S_q \end{bmatrix} \tag{7}$$

The mathematical model expression shown in the Equation (5) can be rewritten as follows after the discretization.

$$\begin{cases} L\frac{i_d(k+1)-i_d(k)}{T_s} & +Ri_d(k+1) = \omega L i_q(k+1) \\ & -e_d(k+1) + \frac{2}{3}U_{DC}(k+1)S_d(k+1) \\ L\frac{i_q(k+1)-i_q(k)}{T_s} & +Ri_q(k+1) = -\omega L i_d(k+1) \\ & -e_q(k+1) + \frac{2}{3}U_{DC}(k+1)S_q(k+1) \end{cases} \tag{8}$$

where T_s is the length of control period, and ω is the angular frequency. In this expression, all of the variables, including the switching state variables, are of DC system and will not change greatly between successive two steps. Therefore, the following expression can be obtained.

$$\begin{cases} U_{DC}(k+1) \approx U_{DC}(k) \\ e_d(k+1) \approx e_d(k) \\ e_q(k+1) \approx e_q(k) \end{cases} \tag{9}$$

Obviously, the minimum value of cost function J can be obtained when satisfying following conditions

$$\begin{cases} i_d(k+1) = i_{dref} \\ i_q(k+1) = i_{qref} \end{cases} \tag{10}$$

Taking above values into the model expression, the switching state variables can be calculated as

$$\begin{cases} S_d(k+1) = \dfrac{e_d(k)+R_p i_{dref}(k)-\omega L_p i_{qref}(k)+L_p \frac{i_{dref}(k)-i_d(k)}{T_s}}{\frac{2}{3}U_{DC}(k)} \\ S_q(k+1) = \dfrac{e_q(k)+R_p i_{qref}(k)+\omega L_p i_{dref}(k)+L_p \frac{i_{qref}(k)-i_q(k)}{T_s}}{\frac{2}{3}U_{DC}(k)} \end{cases} \tag{11}$$

This is the expression to calculate the optimal switching states of the next period. In this expression, the model parameters R_p and L_p are of predicted values and will be modified online. During every control period, the measured variables of currents, voltage are used to calculate the switching state variables. In this method, only above expressions are needed to obtain the optimal switching states. As a result, the computation is reduced comparing with other FCS-MPC inverter control methods.

3.2. Modulation

In this A-MPC current control method, conventional PWM modulation technique can be applied to generate the commands for the switches. The instantaneous values of three-phase inverter switching states variables S_a, S_b and S_c are defined as 1 when the upper switch is on, and as 0 when it is off. Therefore, the equivalent sinusoidal switching state variable in three-phase coordinate system is with a DC bias of 0.5. For the modulation process, the output D_a, D_b and D_c must meet following requirements: (i) The values in two-phase rotating coordinate system of the switching variables are equal to S_d and S_q, and (ii) The DC bias of switching variables is 0.5.

The two basic signals of the modulation process are modulation wave and carrier wave. The modulation wave can be obtained by transforming the switch state variables (S_d and S_q) from rotating coordinate system to three-phase coordinate system (dq to abc). Assuming that during a switch period the range of carrier is set as $[-M, M]$ and the value of modulation wave is A, as shown in Figure 4, the duty cycle of this switch period is

$$D = \frac{A+M}{2M} = \frac{A}{2M} + 0.5 \tag{12}$$

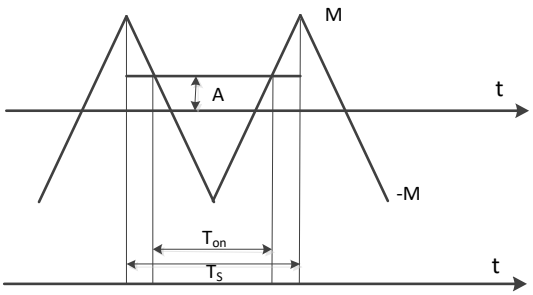


Figure 4. Carrier and modulation waves of PWM modulation.

When M = 0.5, D = A + 0.5, the DC component of the modulation output is 0.5. Therefore, the carrier wave is ranged from −0.5 to 0.5. The modulation process helps increase the numbers of switching states in one period, comparing with other FCS-MPC based methods. In FCS-MPC method, the switching state keeps constant in one control period, and only one switching state, which minimizes the cost function, is selected [23]. As a result, the error of output current is inevitable. In contrast, PWM modulation process can provide more than one switching state and their duty cycle [24]. FCS-MPC methods can only select the switching state with the least current error, resulting in variable switching

frequency and complicated harmonic content [24]. In summary, the modulation method can achieve constant switching frequency and reduce harmonics.

3.3. Parameters Modification

The initial values of model parameters are given according to the acquired information about the inverter. However, in many cases the actual parameters are unavailable, especially in complex systems, and keep changing [25]. Therefore, the model parameters need to be updated online during the control process continuously to ensure the accuracy of the control result.

The action of parameters modification is conducted only when the inverter has been in steady state. In this case the following condition has to be satisfied

$$\begin{cases} L\frac{di_d}{dt} = 0 \\ L\frac{di_q}{dt} = 0 \end{cases} \tag{13}$$

The expression of this operation state in two-phase rotating coordinate system can be rewritten as followings:

$$\begin{cases} Ri_d = \omega L i_q - e_d + \frac{2}{3}U_{DC}S_d \\ Ri_q = -\omega L i_d - e_q + \frac{2}{3}U_{DC}S_q \end{cases} \tag{14}$$

The above expression is about the state of the inverter and is satisfied in any operation situation. The parameters L and R in (12) are both actual physical parameters. When the switching states (11) are substituted into above state equation, it can be rewritten as

$$\begin{cases} Ri_d(k) = & \omega L i_q(k) + R_P(k-1)i_{dref} \\ & -\omega L_P(k-1)i_{qref} + L_P(k-1)\frac{i_{dref}-i_d(k-1)}{T_s} \\ Ri_q(k) = & -\omega L i_d(k) + R_P(k-1)i_{qref} \\ & +\omega L_P(k-1)i_{dref} + L_P(k-1)\frac{i_{qref}-i_q(k-1)}{T_s} \end{cases} \tag{15}$$

It can be seen that both the actual parameter values L and R and the predicted values L_p and R_p have effect on the operation state of the inverter. Since it is under steady state, following expressions are true.

$$\begin{cases} i_d(k-1) = i_d(k) \\ i_q(k-1) = i_q(k) \end{cases} \tag{16}$$

In this case, (15) can be simplified as

$$\begin{cases} Ri_d(k) = & \omega L i_q(k) + R_P i_{dref} - \omega L_P i_{qref} \\ & +L_P\frac{i_{dref}-i_d(k)}{T_s} \\ Ri_q(k) = & -\omega L i_d(k) + R_P i_{qref} + \omega L_P i_{dref} \\ & +L_P\frac{i_{qref}-i_q(k)}{T_s} \end{cases} \tag{17}$$

In above expression, the unknowns are the L and R. Therefore, the actual values of parameters can be obtained by solving this equation.

Firstly, a series of variables are defined as followings:

$$\begin{cases} \zeta_1 = i_d i_{qref} - i_q i_{dref} \\ \zeta_2 = i_d i_{dref} + i_q i_{qref} \\ \zeta_3 = i_d^2 + i_q^2 \end{cases} \tag{18}$$

The expression about parameter L is shown as following

$$L = \frac{(R_P(k-1) + \frac{L_P(k-1)}{T_S})\zeta_1 + \omega L_P(k-1)\zeta_2}{\omega\zeta_3} \tag{19}$$

According to above analysis, the actual parameter at any state can be calculated by the measured data and the predicted model parameters. However, it is not an acceptable way to improve the accuracy of the predicted parameters by setting L_p equal to L directly. This is because the change of L_p or R_p will cause the change of inverter operation state, and then change the actual value of the parameters. Furthermore, a dramatic change of parameters may have a negative impact on the stability or power quality of inverter current. Therefore, the method of step by step approximation is adopted here. The difference between L and L_p can be expressed as

$$L - L_P = \frac{(R_P + \frac{L_P}{T_S})\zeta_1 + \omega L_P(\zeta_2 - \zeta_3)}{\omega\zeta_3} \tag{20}$$

Similarly, the difference between R and R_p can be calculated as

$$R - R_P = \frac{-\omega L_P\zeta_1 + \frac{L_P}{T_S}(\zeta_2 - \zeta_3) + R_P(\zeta_2 - \zeta_3)}{\zeta_3} \tag{21}$$

Above expressions can be used to modify the predicted model parameters. When the inverter has been in stable operation state, the accuracy of the output current is estimated. If the error between reference and measured current is larger than the maximum permissible value, the action of parameters modification will be conducted. The parameters can be modified according to following expressions.

$$\begin{cases} L_P(k) = L_P(k-1) + \Delta L & if \quad L - L_P > \varepsilon_L \\ L_P(k) = L_P(k-1) - \Delta L & if \quad L - L_P < -\varepsilon_L \\ L_P(k) = L_P(k-1) & if \quad -\varepsilon_L < L - L_P < \varepsilon_L \end{cases} \tag{22}$$

$$\begin{cases} R_P(k) = R_P(k-1) + \Delta R & if \quad R - R_P > \varepsilon_R \\ R_P(k) = R_P(k-1) - \Delta R & if \quad R - R_P < -\varepsilon_R \\ R_P(k) = R_P(k-1) & if \quad -\varepsilon_R < R - R_P < \varepsilon_R \end{cases} \tag{23}$$

where ΔL and ΔR are the unit changes of inductance and resistance respectively. ε_L and ε_R are the maximum acceptable errors of inductance and resistance respectively. The complete scheme of the proposed A-MPC current control process is given in Figure 5.

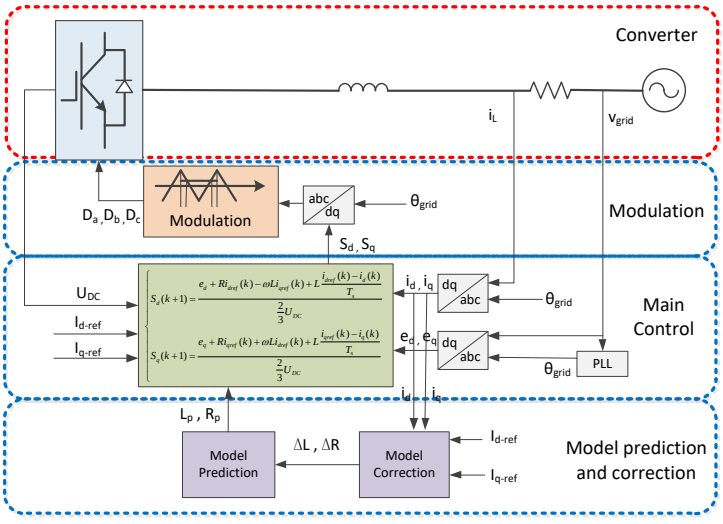


Figure 5. Complete scheme of the proposed control method.

4. Simulation and Experimental Results

The proposed A-MPC based inverter control method has been validated through simulation and experiments. Firstly, a series of simulations through MATLAB/Simulink are conducted to compare the performances of common FCS-MPC based inverter control method and the proposed method. In order to take the simulation and experiments to a close agreement, the simulation model of the three-phase inverter is established according to the practical experiment parameters, which is listed as Table 1.

Table 1. Parameters of Simulation.

Parameters	Symbol	Value	Unit
Voltage of grid	V_{AC}	380	V
Voltage of DC bus	V_{DC}	600	V
Fundamental frequency	f	50	Hz
Rated power of inverter	P_{rated}	10	kW
Filter inductor	L_f	1.5	mH
Switching frequency	f_s	6	kHz

As mentioned, in existing FCS-MPC based inverter control methods, the switching variables are directly selected according to the cost function by comparing all the possible variables, known as exhaustive method. There are three obvious drawbacks mentioned above. To address these three issues, this paper proposes A-MPC inverter current control method. The proposed method can overcome these problems effectively.

In order to validate it, two groups of simulations are conducted and the results are compared. The output current waveforms of the FCS-MPC method and proposed method are shown in Figures 6 and 7 respectively. As seen in the figures, the total harmonic distortion (THD) of the proposal (4.71%) is obviously lower than that of common FCS-MPC (12.19%), owing to the modulation process.

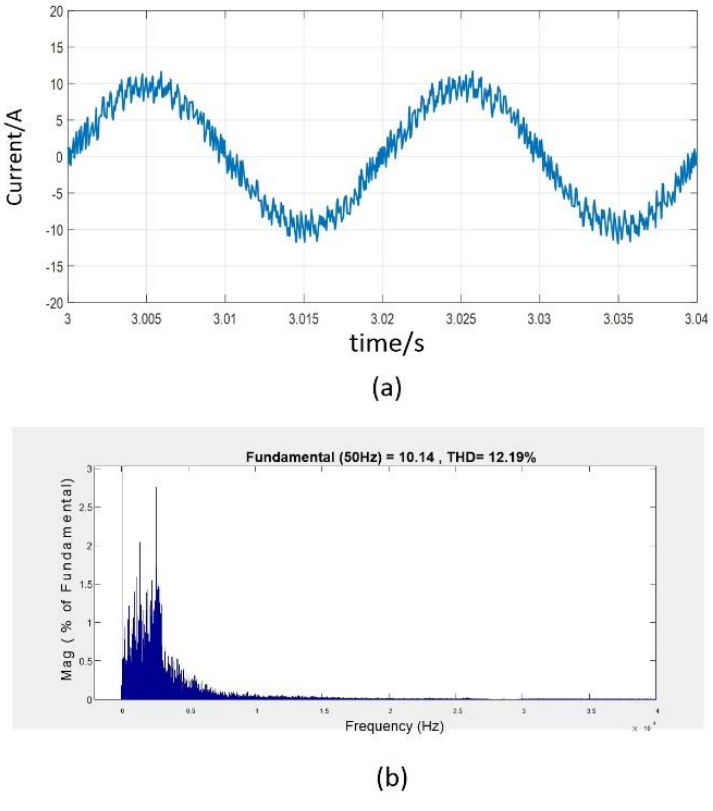
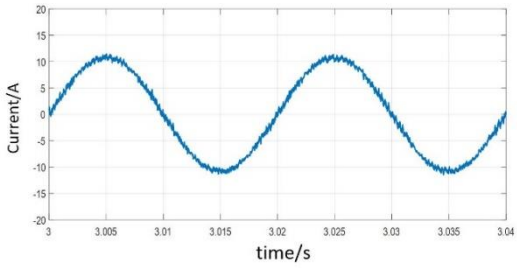
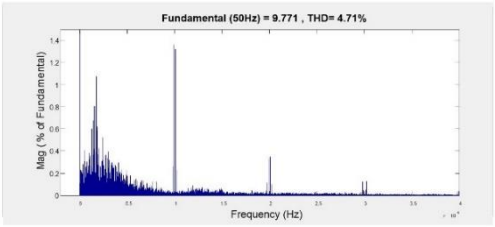


Figure 6. Simulation results for the output current waveforms of FCS-MPC (**a**) current waveform for 0.04 s, (**b**) current THD.



(a)



(b)

Figure 7. Simulation results for the output current waveforms of the proposed A-MPC (**a**) current waveform for 0.04 s, (**b**) current THD.

Since the A-MPC method removes the process of evaluating all the optional switching states, the computation is reduced. During above simulations, the processing time of each method is shown in Figure 8. The total recorded time of simulation under control of the proposal (265.62 s) is less than that of FCS-MPC based method (338.16 s). The listed total recorded time includes both the time cost by the control method and by other parts of the simulation model. Since there is no difference in the inverter models of each simulation, all of the reduced time (72.54 s) is caused by the simplification of control method. Therefore, the computation reduction in control method is significant.

Simulink Profile Report: Summary

Report generated 10-Sep-2017 22:14:35

Total recorded time:	265.62 s
Number of Block Methods:	1124
Number of Internal Methods:	6
Number of Model Methods:	13
Number of Nonvirtual Subsystem Methods:	76
Clock precision:	0.00000004 s
Clock Speed:	2501 MHz

To write this data as inverterMPC08ProfileData in the base workspace click here

(a)

Simulink Profile Report: Summary

Report generated 10-Sep-2017 22:45:15

Total recorded time:	338.16 s
Number of Block Methods:	618
Number of Internal Methods:	6
Number of Model Methods:	15
Number of Nonvirtual Subsystem Methods:	72
Clock precision:	0.00000004 s
Clock Speed:	2501 MHz

To write this data as MPC2ProfileData in the base workspace click here

(b)

Figure 8. Comparison of simulation time between the proposed method and FCS-MPC based method (**a**) recorded time of the A-MPC based method, (**b**) recorded time of the FCS-MPC based method.

In order to analyze the performance of this MPC based control method under grid transients, a group of simulations are conducted on the condition of single-phase ground fault. The current of inverter are shown in Figure 9. It can be seen the amplitude of current changes during this period and its THD increases. Although the fault has negative effect on the power quality, the current is under control and return to stable state after the fault is eliminated. The performance of the proposed method is similar to that of other control method, such as PI control.

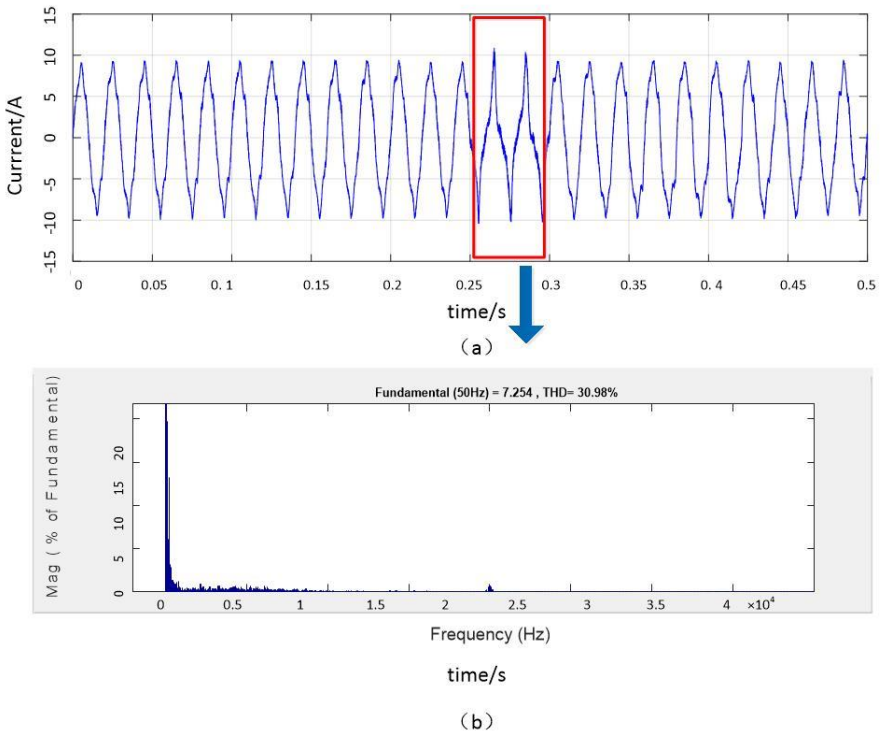


Figure 9. Current performance under single-phase ground fault (**a**) current waveform (**b**) THD of current within the fault period.

In order to verify the effectiveness of the proposal in practical applications and compare the performances with other traditional control methods, a series of experiments are conducted in a microgrid laboratory, as shown in Figure 10. Parameters of the controlled inverter and other devices of the experimental system are shown as Table 1. The experimental result is collected by ScopeCorder DL850E, which combines a mixed oscilloscope and data acquisition recorder. In this way, the collected data can be inputted into a computer and processed.



Figure 10. Microgrid laboratory.

Firstly, a group of experiments are conducted aiming to show validity of the model parameters modification process in the proposal. At the beginning the predicted parameters are given as L = 0.8 mH and R = 3 Ω, and reference RMS of output current is 10 A. The modification action is performed once every 0.1 s. Recorded output current during the modification process is shown in Figure 11a, while its RMS waveform is shown in Figure 11b, which is calculated by computer. It can be seen the accuracy of RMS of the output current is continuously improved with the modification. When the error between reference and collected current is less than the threshold, the modification is stopped, and will not be started until the error is larger than the threshold.

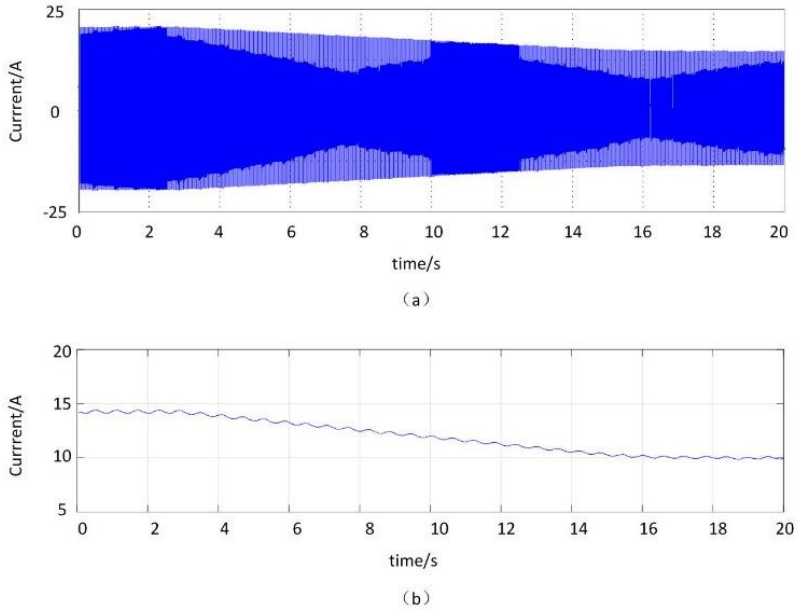


Figure 11. Experimental results for model parameters modification process of the proposed method (**a**) Current waveform, (**b**) current RMS waveform.

In this system, the control frequency 6 kHz is relatively low because of the limit by the switching frequency of inverter. In order to verify the effectiveness of the proposed A-MPC based method in such a practical application, the steady state performance is analyzed. When the inverter is operated in a stable state, the current waveform and its THD are shown in Figure 12. The THD 4.70%, can satisfy the current harmonics requirement of IEEE standard IEEE1547 [26].

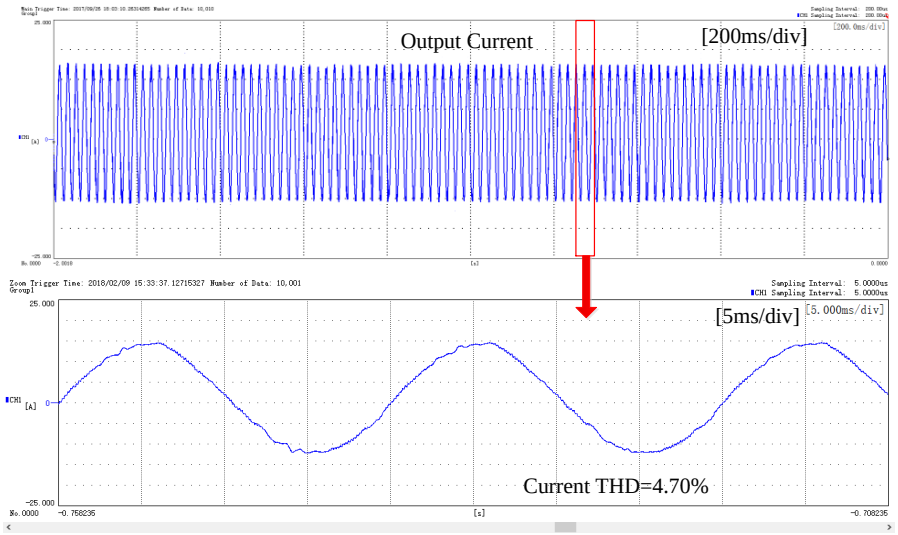


Figure 12. Experimental results for steady-state current of the proposed A-MPC based method.

To analyze dynamic performance of the proposal, another group of experiments is carried out. During the experiment, the reference current RMS changed from 5A to 10A at some moment. This test is carried out in order to compare the response speed and output current overshoot under step change. When the inverter is operated under PI control, the current waveform and its RMS waveform are presented in Figures 13a and 13b respectively

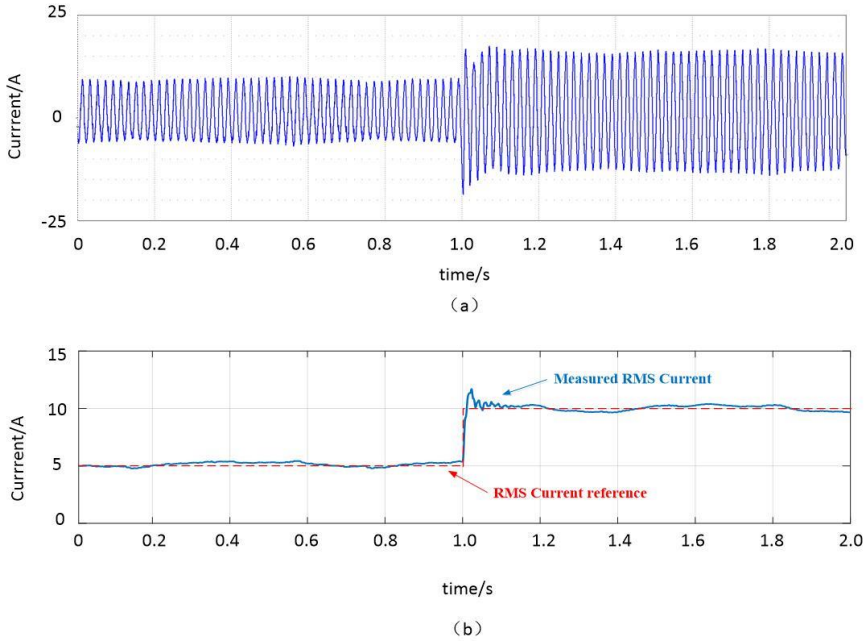


Figure 13. Experimental results for step current of PI control (**a**) real-time current waveform, (**b**) RMS current.

When the inverter is operated under PR control, the step current waveform and its RMS waveform are presented in Figure 14a,b respectively.

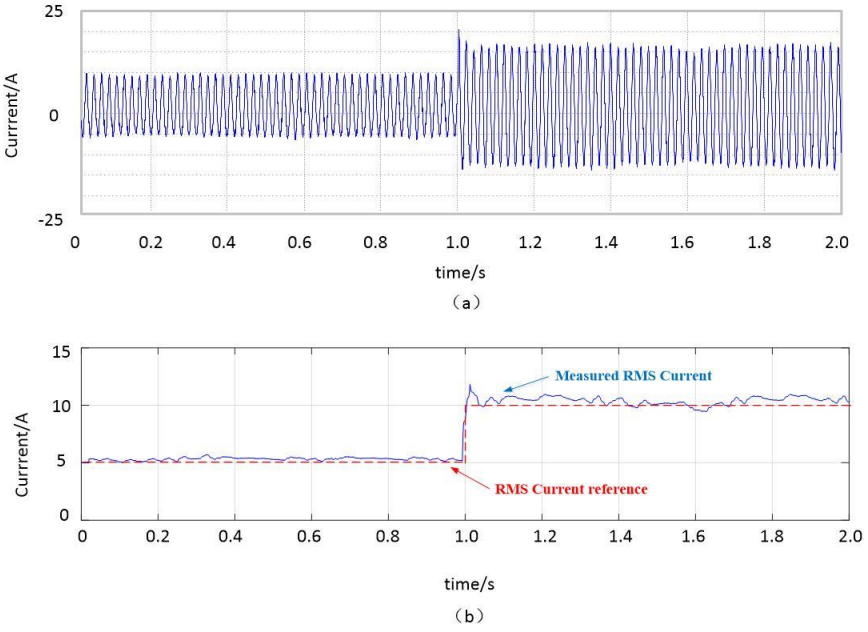


Figure 14. Experimental results for step current of PR control (**a**) real-time current waveform, (**b**) RMS current.

The response of the proposed A-MPC based control method to the same change is shown in Figure 15a,b. Since the testing time is long, above waveform, which spans 2 s, is just a part of the whole current waves. That is why the step change time in these two figures are different.

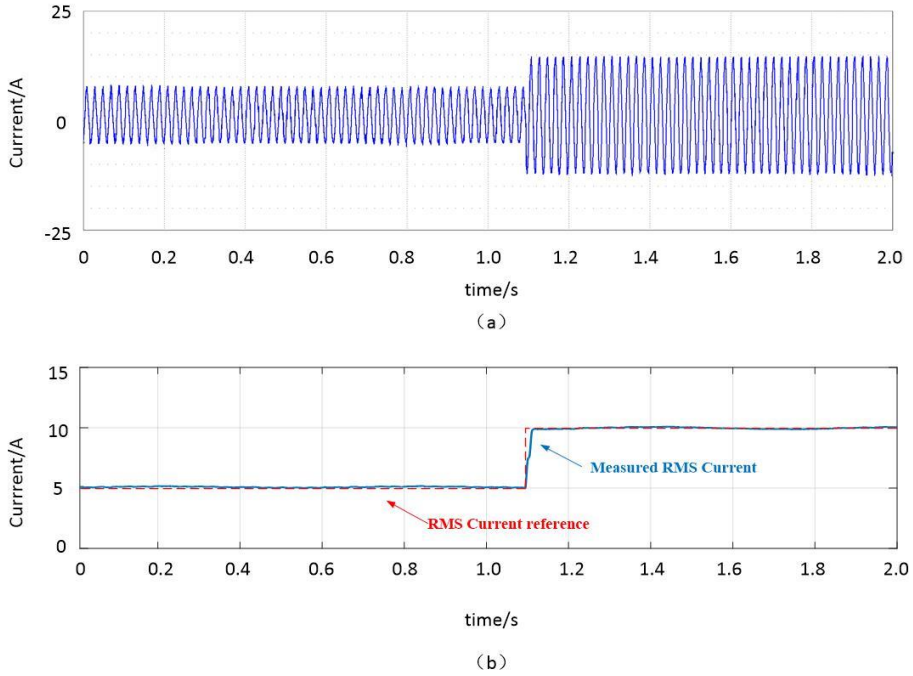


Figure 15. Experimental results for step current of the proposed A-MPC control method (**a**) real-time current waveform, (**b**) RMS current.

As shown in the figures, the response speed of the proposal to step change is much higher than that of PI and PR control. At the same time, the current overshoot is also reduced substantially in this A-MPC method. Generally, in many of traditional control methods, such as PI and PR control, the response speed and overshoot are two conflicting goals when designing control parameters. By using the proposal in controlling an inverter, both these performances are improved. Therefore, this method has significant advantages in applications with frequent change of current, such as photovoltaic inverters and energy storage converters.

5. Conclusions

In this paper, an A-MPC based current control for three-phase converters is proposed. This approach takes use of inverter mathematical model in two-phase rotating coordinate system to calculate the optimal switching state in each cycle. Comparing to existing FCS-MPC based inverter control methods, the proposed method reduces the computational burden and control complexity, and improves power quality. A parameter estimation and adaptive control method is also integrated into the proposed method. The overall control scheme is straightforward and simple to implement. Experimental results are presented to validate the improvement of dynamic performances. Comparing to conventional PI and PR control, the response speed of the A-MPC is faster and the overshoot is smaller. Future research aims to apply the method to other converter topologies, e.g., modular multi-level converters, etc.

Author Contributions: Conceptualization, M.L.; methodology, M.L. and L.M.; software, Z.Y.; validation, M.L., Y.Z. and D.C.; formal analysis, Z.Y.; investigation, L.M.; resources, M.L. and Z.Y.; data curation, M.L.; writing—original draft preparation, M.L. and L.M.; writing—review and editing, M.L.; visualization, Y.Z.; supervision, Y.W.; project administration, Y.W.; funding acquisition, Y.W.

Funding: This research was funded by Qinghai Science and Technology Project "Key technologies for renewable energy and energy storage integration applications": 2019-GX-A9

Conflicts of Interest: The authors declare no conflict of interest.

References

1. Kouro, S.; Cortes, P.; Vargas, R.; Ammann, U.; Rodriguez, J. Model predictive control—A simple and powerful method to control power converters. *IEEE Trans. Ind. Electron.* **2009**, *56*, 1826–1838. [CrossRef]
2. Camacho, D.E.F.; Bordons, D.C. *Model Predictive Control*; Springer: London, UK, 2007; pp. 575–615.
3. Mariethoz, S.; Morari, M. Explicit Model-Predictive Control of a PWM Inverter with an LCL Filter. *IEEE Trans. Ind. Electron.* **2009**, *56*, 389–399. [CrossRef]
4. Cortes, P.; Ortiz, G.; Yuz, J.I. Model Predictive Control of an Inverter with Output LC Filter for UPS Applications. *IEEE Trans. Ind. Electron.* **2009**, *56*, 1875–1883. [CrossRef]
5. Nauman, M.; Hasan, A. Efficient Implicit Model-Predictive Control of a Three-Phase Inverter with an Output LC Filter. *IEEE Trans. Power Electron.* **2016**, *31*, 6075–6078. [CrossRef]
6. Guzman, R.; Vicuna, L.G.D.; Camacho, A.; Miret, J.; Rey, J.M. Receding-Horizon Model Predictive Control for a Three-Phase VSI with an LCL Filter. *IEEE Trans. Ind. Electron.* **2018**, *99*, 6671–6680. [CrossRef]
7. Lee, J.H.; Lee, J.S.; Moon, H.C.; Lee, K.B. An Improved Finite Set Model Predictive Control Based on Discrete Space Vector Modulation Methods for Grid-Connected Three-Level Voltage Source Inverter. *IEEE J. Emerg. Sel. Top. Power Electron.* **2018**, *6*, 1744–1760. [CrossRef]
8. Moon, H.C.; Lee, J.S.; Lee, K.B. A Robust Deadbeat Finite Set Model Predictive Current Control Based on Discrete Space Vector Modulation for Grid-Connected Voltage Source Inverter. *IEEE Trans. Energy Convers.* **2018**, *33*, 1719–1728. [CrossRef]
9. Vatani, M.; Bahrani, B.; Saeedifard, M. Indirect Finite Control Set Model Predictive Control of Modular Multilevel Converters. *IEEE Trans. Smart Grid.* **2015**, *6*, 1520–1529. [CrossRef]
10. Ghanes, M.; Trabelsi, M.; Abu-Rub, H. Robust Adaptive Observer-Based Model Predictive Control for Multilevel Flying Capacitors Inverter. *IEEE Trans. Ind. Electron.* **2016**, *63*, 7876–7886. [CrossRef]
11. Xia, C.; Liu, T.; Shi, T.; Song, Z. A Simplified Finite-Control-Set Model-Predictive Control for Power Converters. *IEEE Trans. Ind. Informat.* **2017**, *10*, 991–1002.
12. Zhang, Y.; Qu, C. Model Predictive Direct Power Control of PWM Rectifiers under Unbalanced Network Conditions. *IEEE Trans. Ind. Electron.* **2015**, *62*, 4011–4022. [CrossRef]
13. Errouissi, R.; Muyeen, S.M.; Al-Durra, A.; Leng, S. Experimental Validation of Robust Continuous Nonlinear Model Predictive Control Based Grid-Interlinked Photovoltaic Inverter. *IEEE Trans. Ind. Electron.* **2016**, *63*, 4495–4505. [CrossRef]
14. Errouissi, R.; Ouhrouche, M.; Chen, W.H.; Trzynadlowski, A.M. Robust cascaded nonlinear predictive control of a permanent magnet synchronous motor with antiwindup compensator. *IEEE Trans. Ind. Electron.* **2012**, *59*, 3078–3088. [CrossRef]
15. Rodríguez, J.; Pontt, J.; César, A.; Pablo Correa, S.; Lezana, P.; Cortés, P.; Ammann, U. Predictive Current Control of a Voltage Source Inverter. *IEEE Trans. Ind. Electron.* **2007**, *54*, 495–503. [CrossRef]
16. Metri, J.I.; Vahedi, H.; Kanaan, H.Y.; Al-Haddad, K. Real-Time Implementation of Model-Predictive Control on Seven-Level Packed U-Cell Inverter. *IEEE Trans. Ind. Electron.* **2016**, *63*, 4180–4186. [CrossRef]
17. Garcia, C.F.; Rivera, M.E.; Rodríguez, J.R. Predictive Current Control With Instantaneous Reactive Power Minimization for a Four-Leg Indirect Matrix Converter. *IEEE Trans. Ind. Electron.* **2017**, *64*, 922–929. [CrossRef]
18. Ma, Z.; Saeidi, S.; Kennel, R. FPGA implementation of model predictive control with constant switching frequency for PMSM drives. *IEEE Trans. Ind. Inform.* **2014**, *10*, 2055–2063. [CrossRef]
19. Young, H.A.; Perez, M.A.; Rodriguez, J. Analysis of Finite-Control-Set Model Predictive Current Control with Model Parameter Mismatch in a Three-Phase Inverter. *IEEE Trans. Ind. Electron.* **2016**, *63*, 3100–3107. [CrossRef]
20. Li, X.; Shamsi, P. Model Predictive Current Control of Switched Reluctance Motors With Inductance Auto-Calibration. *IEEE Trans. Ind. Electron.* **2016**, *63*, 3934–3941. [CrossRef]
21. Cherif, A.Y.; Remache, S.E.I.; Barra, K.; Wira, P. Adaptive Model Predictive Control for Three Phase Voltage Source Inverter using ADALINE estimator. In Proceedings of the 1st Global Power, Energy and Communication Conference, Nevsehir, Turkey, 12–15 June 2019.

22. Blasko, V.; Kaura, V. A new mathematical model and control of a three-phase AC-DC voltage source converter. *IEEE Trans. Power Electron.* **2002**, *12*, 116–123. [CrossRef]
23. Pollmann, A.J. Software pulse width modulation for up control of AC drives. *IEEE Trans. Indus. Appl.* **1986**, *22*, 519–524.
24. Wang, X.; Blaabjerg, F.; Wu, W. Modeling and Analysis of Harmonic Stability in an AC Power-Electronics-Based Power System. *IEEE Trans. Power Electron.* **2014**, *29*, 6421–6432. [CrossRef]
25. Rodriguez, J.; Cortes, P. *Predictive Control of Power Converters and Electrical Drives*; John Wiley & Sons: Hoboken, NJ, USA, 2012.
26. IEEE. *IEEE Standard for Interconnecting Distributed Resources with Electric Power Systems*; IEEE Std 1547–2018; IEEE: Piscataway, NJ, USA, 2003.



© 2019 by the authors. Licensee MDPI, Basel, Switzerland. This article is an open access article distributed under the terms and conditions of the Creative Commons Attribution (CC BY) license (http://creativecommons.org/licenses/by/4.0/).